



Upgrading of Napier grass pyrolytic oil using microporous and hierarchical mesoporous zeolites: Products distribution, composition and reaction pathways



Isah Yakub Mohammed^{a, b, g, *}, Yousif Abdalla Abakr^c, Suzana Yusup^d, Peter Adeniyi Alaba^e, Kenobi Isima Morris^c, Yahaya Muhammad Sani^e, Feroz Kabir Kazi^f

^a Department of Chemical and Environmental Engineering, The University of Nottingham Malaysia Campus, Jalan Broga, Semenyih 43500, Selangor Darul Eshan, Malaysia

^b Department of Chemical Engineering, Abubakar Tafawa Balewa University, P.MB 0248, Bauchi, Nigeria

^c Department of Mechanical, Manufacturing and Material Engineering, The University of Nottingham Malaysia Campus, Jalan Broga, Semenyih 43500, Selangor Darul Eshan, Malaysia

^d Department of Chemical Engineering, Universiti Teknologi PETRONAS, Bandar Seri Iskandar, 31750 Tronoh, Malaysia

^e Department of Chemical Engineering, University of Malaya, Kuala Lumpur 50603, Malaysia

^f Department of Engineering and Mathematics, Sheffield Hallam University, City Campus, Howard Street, Sheffield S1 1WB, UK

^g Crops for the Future (CFF), The University of Nottingham Malaysia Campus, Jalan Broga, Semenyih 43500, Selangor Darul Eshan, Malaysia

ARTICLE INFO

Article history:

Received 11 August 2016

Received in revised form

12 June 2017

Accepted 12 June 2017

Available online 14 June 2017

Keywords:

Napier grass

Pyrolytic oil

Deoxygenation

Reaction pathways

Microporous ZSM-5

Mesoporous ZSM-5

Hydrocarbons

ABSTRACT

Reaction pathways in *ex-situ* catalytic upgrading of pyrolytic oil towards formation of specific products such as hydrocarbons are still not well established due to the presence of many different organic components in the raw pyrolytic oil. Currently, only a few studies are available in literature particularly with regards to application of hierarchical mesoporous zeolite in the refinement of sample pyrolytic oil. This study provides the first experimental investigation of *ex-situ* catalytic upgrading of pyrolytic oil derived from Napier grass using microporous and hierarchical mesoporous zeolites. Two hierarchical mesoporous zeolites were synthesized by desilication of microporous zeolite using 0.2 and 0.3 M solution of sodium hydroxide. Upgrading over microporous zeolite produced 16.0 wt% solid, 27.2 wt% organic phase and 23.9 wt% aqueous phase liquid while modified zeolites produced 21–42% less solid and 15–16% higher organic phase liquid. Higher degree of deoxygenation of pyrolytic oil was achieved with the modified zeolites. Analysis of organic phase collected after catalytic upgrading revealed high transformation of oxygenates into valuable products. Bulk zeolite produced cyclic olefins and polyaromatic hydrocarbons while mesoporous zeolites were selective toward cycloalkanes and alkylated monoaromatic production, with significant reduction in the production of polyaromatic hydrocarbon. Result of gas analysis showed that hierarchical mesoporous zeolite favored decarboxylation and decarbonylation reactions compared to the parent zeolite, which promoted dehydration reaction. Mesoporous zeolite produced with 0.3 M sodium hydroxide solution was found to be the best-performing catalyst and its reusability was tested over four consecutive cycles. This study demonstrated that pyrolytic oil derived from Napier grass can be transformed into high-grade oil over hierarchical mesoporous zeolite.

© 2017 Elsevier Ltd. All rights reserved.

* Corresponding author. Department of Chemical and Environmental Engineering, The University of Nottingham Malaysia Campus, Jalan Broga, Semenyih 43500, Selangor Darul Eshan, Malaysia.

E-mail addresses: yimohd@atbu.edu.ng, kebx3iye@nottingham.edu.my (I.Y. Mohammed).

1. Introduction

Development of an alternative fuel that would replace or reduce dependency on the fossil based fuels continues to gain attention in recent times due to the fear of energy insecurity in the near future and environmental impact associated with the use of petroleum-based fuels in addition to sociopolitical issues (Yakub et al., 2015). Lignocellulosic biomass (non-food materials: forest residues, agro-

wastes, energy grasses), and aquatic plants and algae are being considered as alternative feedstock for the production of renewable biofuel due to the presence of carbon in their building blocks, which can be processed into liquid fuel (Mohammed et al., 2015). Pyrolysis remains an attractive route for the thermochemical conversion of biomass as it comprises fewer steps and capable of high liquid yield (known as pyrolysis oil or pyrolytic oil) through a careful control of process parameters such pyrolysis temperature, heating rate, vapor residence time in the reactor, and rapid cooling of the volatile in the condenser (Mohammed et al., 2016). Pyrolytic oil from biomass is a complex mixture consisting predominantly oxygenated organic compounds, phenolics, light hydrocarbons and traces of nitrogen and sulfur containing compounds depending on nature of the source biomass. The high level of the oxygenated compound in the oil is responsible for the poor physicochemical characteristics such as low pH, low chemical stability, low energy content (Mohammed et al., 2016). This therefore rendered the oil unsuitable for direct application as fuel or refinery-ready feedstock for quality fuel production and other consumer products.

Catalytic upgrading of pyrolytic oil is one of the techniques being used to improve the quality of the oil. This approach provides more process flexibility as the upgrading step can be manipulated and optimized individually. Catalytic cracking of pyrolysis oil over porous materials such as zeolite (HY, mordenite, silica-alumina, silicalite, ZSM-5) is now receiving more attention. ZSM-5 (MFI-Mordenite Framework Inverted) is a microporous material in nature with a well-defined pore structure and acidity, which selectively allows diffusion and conversion of molecules (Mante et al., 2014). Study by Vitolo et al. (2001) on the catalytic cracking of pyrolysis oil produced from wood with ZSM-5 (2 g) at temperature between 410 and 450 °C in a fixed bed micro-reactor with a feed flow rate of 5.9 mL/h revealed that upgrading reactions such as decarboxylation, decarbonylation, cracking, aromatization, alkylation, isomerisation, cyclisation and oligomerization proceed via carbonium ion mechanism, which occurred at the acidic sites (Brønsted acid sites) of the ZSM-5. Coke and tar were also observed as co-products from the catalytic reaction, which led to the catalyst poisoning. The upgraded products recorded with fresh ZSM-5 was 11.3 wt% organics, 28.9 wt% aqueous, 47.7 wt% non-condensable gas and 11 wt% solid. High yield of the non-condensable gas recorded was attributed to high degree of deoxygenation reactions. Recently, Saad et al. (2015) reported catalytic cracking of pyrolysis oil derived from rubber wood in a dual reactor using ZSM-5 (3.2 g) at 511 °C with feed rate of 1.4 g/min. They observed the highest organic product yield of 13.36 wt% with 44.93 wt% aqueous phase. Despite the use of dual reactor system, which was meant to reduce coke formation, solid product as high as 29.2 wt% was recorded. They concluded that the low yield of upgraded organic product was due to poor physicochemical properties of the raw pyrolysis oil used. This could also be linked to oxygen-containing chemical species such as guaiacols, furanic rings and sugars in the pyrolysis oil, which are perceived to result in coke formation during upgrading due to their instability and deficiency in molar balance (Zhang et al., 2014). The coke precursors are said to undergo polymerization and polycondensation on the catalytic surface, fill up the inner pores and eventually result in the catalyst deactivation (Wei et al., 2016). Researchers have suggested that lignin-derived compounds are more susceptible to char and coke formation during cracking and upgrading of pyrolytic oil derived from lignocellulosic biomass compared to compounds from hemicellulose and cellulose (acid, aldehydes, ketones, ester, and sugars). This was attributed to the complex structure and bulkiness of the lignin derivatives, which make them too large for the pores of the ZSM-5 catalyst (Zhang et al., 2015). Recent studies by Wei et al. (2016) on catalytic cracking of pure phenol and guaiacol as model compounds over

ZSM-5 revealed that less catalytic coke was formed with the model compounds compared to the pyrolysis oil. They proposed that there are possible interactions between the derivatives of hemicellulose and cellulose with the lignin-derived compounds during the upgrading reactions. They further investigated cracking of pure pyrolysis oil mixed with 50 wt% methanol and phenolic-rich pyrolysis oil fraction mixed with methanol in order to evaluate the ZSM-5 coking condition and hydrocarbon yield. The result showed that the later feedstock produced more hydrocarbon and less coke compared to the former. They concluded that small active molecules are also responsible for the catalyst coking by adhering to the active sites in the pores.

Studies aimed at minimizing catalyst deactivation is as old as the catalytic process development and searching for long-lasting solutions are in progress to ensure industrial process scale-up (Alaba et al., 2016a). Structural modification of zeolite is being given considerable attention in recent time as a solution to coke formation by diffusion limitation (García et al., 2015). Researchers have shown that modification (demetalation) of zeolite in an alkaline medium produced a partial collapse of the zeolite network into more than one level of porosity (micro and mesoporosity) with a network of interconnected cavities and cylindrical channels located in both outer and inner portions of the zeolite crystals (Na et al., 2013). The resulting solid from the alkaline treatment tends to exhibit significantly enhanced accessibility of the active site, remarkable hydrothermal stability and longevity of the catalyst as a result of reduction in size of the purely microporous domains and facile diffusion of coke precursors through the mesopore, in addition to retaining the other zeolitic properties of its parent material (García et al., 2015). This method is therefore considered as an attractive top-down approach for the development of hierarchical zeolites with superior properties to meet their applications in catalytic cracking processes, particularly in the area of pyrolytic oil upgrading for development of alternative renewable biofuel (Pérez-Ramírez et al., 2011).

Application of hierarchical mesoporous ZSM-5 in catalytic deoxygenation of pyrolysis vapor have shown significant improvement in the quality of pyrolysis oil (Lee et al., 2014; Li et al., 2014b; Gamiel et al., 2016; Mohammed et al., 2017a). For ex-situ upgrading studies over hierarchical mesoporous ZSM-5, most researchers have focused on the use of synthetic or model pyrolytic oil compounds as a basis for evaluating the catalyst performance (Botas et al., 2014; Tian et al., 2016). Report by Puértolas et al. (2015) is one of the recent studies where upgrading of actual pyrolytic oil was investigated. Pyrolytic oil derived from pine wood was converted to aromatics over bulk (microporous) and hierarchical mesoporous ZSM-5 in a fixed bed reactor at 450 °C. The upgraded pyrolytic oil over mesoporous ZSM-5 exhibited better physicochemical properties relative to the parent ZSM-5. The catalyst promoted the production of monoaromatic hydrocarbon such as benzene, toluene and xylene (BTX) while decrease in the amount of phenolics, acids, ketones was observed. The formation of aromatics was linked to the increased accessible acid sites present at the mesopore walls and external surface. Higher composition of CO in the non-condensable gas with the mesoporous ZSM-5 was observed compared to the parent ZSM-5. The amount of CO in the gas showed a strong linear relationship with the amount of aromatics in the upgraded pyrolytic oil. The authors concluded that mesoporous ZSM-5 favored decarbonylation reaction compared to the parent ZSM-5, which promoted dehydration reaction. Similarly, Veses et al. (2016) reported deoxygenation of pyrolytic oil derived from wood over metal loaded hierarchical mesoporous ZSM-5. Catalytic activity of metal loaded hierarchical mesoporous ZSM-5 was compared with that mesoporous ZSM-5. The result showed comparable product distribution. Nearly 57 wt% total liquid, 21 wt% gas and 21 wt% char was recorded

with mesoporous ZSM-5 while the metal loaded mesoporous ZSM-5 had 56–60 wt% liquid, 19–22 wt% gas and 19–22 wt% char. Although, maximum organic phase oil yield relative to the feed pyrolytic oil was achieved (41 wt%) with the metal loaded mesoporous ZSM-5 compared to the mesoporous ZSM-5, which produced about 35 wt%. The corresponding degree of deoxygenation achieved was 42.6% and 35%. However, from the result presented by authors, the upgraded oil produced over mesoporous ZSM-5 had lower phenolics, acid, aldehyde and ketones in addition to higher monoaromatic hydrocarbons and lower polyaromatic hydrocarbons. It can be seen that upgraded pyrolytic oil over mesoporous ZSM-5 has higher potential to be converted to fuel and valuable chemicals. The presence of less acid and other oxygenates in the oil are general requirement for avoidance of side reactions during storage, prior to further processing into fuels. Monoaromatics are high valuable chemicals and have commercial application in the petrochemical industry while the low amount of polyaromatic hydrocarbons signifies that the oil is less toxic.

Reaction pathways in ex-situ catalytic upgrading towards formation of specific products such as saturated hydrocarbons, olefins, monoaromatic hydrocarbons are still not well established due to the different organic components in the raw pyrolytic oil. Currently, catalytic upgrading of pyrolytic oil derived from Napier grass has not been reported. This study presents experimental report on ex-situ catalytic upgrading of pyrolytic oil derived from Napier grass over microporous and hierarchical mesoporous ZSM-5 in a high-pressure micro-reactor.

2. Materials and method

2.1. Materials

Crude pyrolytic oil used in this study was organic phase product derived from Napier grass in a vertical fixed bed reactor at 600 °C, 50 °C/min under 5 L/min nitrogen atmosphere. The oil had density and higher heating value on dry basis 0.98 g/cm³ and 29.18 MJ/kg respectively. The consists of 53.87 wt% carbon, 6.45 wt% hydrogen, 1.35 wt% nitrogen, 0.76 wt% sulfur and 37.57 wt% oxygen. Chemical composition of the pyrolytic oil was established using GC-MS analysis. Based on the GC-MS percentage peak area, the oil is made up of 4.67% aliphatic hydrocarbon (ALHC), 2.53% aromatic hydrocarbon (ARHC), 28.15% normal phenol (PHOL), 37.87% methoxy phenol (MTPHOL), 2.18% methoxy aromatic (MARHC), 16.88% acids, ketones, aldehydes (AAK), 3.05% imidazole and 4.68% esters (Mohammed et al., 2017b). Zeolite catalyst was purchased from Fisher Scientific Sdn. Bhd. (Selangor, Malaysia). Sample was taken and converted to protonic form by calcining at 550 °C in air at 5 °C/min for 5 h and the resulting solid was designated as ZSM-5. Hierarchical mesoporous ZSM-5 was obtained from desilication of ZSM-5 using aqueous NaOH solution. 30 g of ZSM-5 was mixed with different aqueous solution (0.2 and 0.3 M) of NaOH (300 mL) for 2 h at 70 °C. The solid was filtered using vacuum filtration with the aid of a polyamide filter and thereafter oven dried at 100 °C. The dried samples were transformed into H-form with 0.2 M NH₄NO₃ solution at 80 °C for 24 h, followed by overnight drying at 100 °C and calcination at 550 °C for 5 h. The final alkaline treated solids were designated as 0.2HZSM-5 and 0.3HZSM-5. Alkaline and acid treatments of zeolite have been reported in the literature but information about the effluents generated from these processes are very limited. In this study, the concentration of NaOH and NH₄NO₃ were carefully selected towards cleaner catalyst synthesis in addition to maintaining the structural integrity and catalytic properties. The leachates generated were channelled to microalgae cultivation unit as part of the nutrients in accordance to Bold's Basal Medium (BB) formulation (Bischoff and Bold, 1963). All the catalysts were characterised according to

standard procedures. X-ray diffraction (PANalytical X'pertPro, DSKH Technology Sdn. Bhd. Selangor, Malaysia) was used to examine the nature of the crystalline system at 2θ angles between 10° and 60°, 25 mA, 45 kV, step size of 0.025°, and 1.0 s scan rate. Scanning electron microscopy (SEM) (FEI Quanta 400 FE-SEM, Hillsboro, USA) was used to evaluate the surface and structural characteristics. Specific surface area and pore properties were determined using physisorption analyzer (ASAP 2020, Micrometrics, Norcross, USA). Acidity of the catalyst was determined via ammonia-temperature programmed desorption (TPD) using a pulse chemisorption system (ChemiSorb 2720, Micrometrics, Norcross, USA).

2.2. Catalytic upgrading

Catalytic upgrading of the crude pyrolysis oil was carried out in a high-pressure reactor. The reactor was a 50 mL stainless steel (SS) Swagelok double-ended (FNPT 6.35 mm) tube (304L SS/DOT-3E 1800 TC-3EM 124) of length 98.6 mm and 2.4 mm wall thickness. The experimental set-up as shown in Fig. 1 consists of the reactor tube, 1/6D series needle valve (SS-16DKM4-F4, 6.35 mm MNPT by 6.35 mm FNPT SS316) attached to a 6.35 mm SS 316 T-piece connected to 6.35 mm fitting from the top of the reactor tube. The remaining end of the T-piece was connected to a reducing adapter (SS-8-RA-4, 12.70 mm FNPT by 6.35 mm MNPT, SS316) attached to a rupture disc (SS-RTM8-F4-2, 12.70 mm MNPT by 6.35 mm FNPT, SS) joined to a 6.35 mm SS extension tube with Skyflex pressure gauge. The bottom of the reactor was closed with 6.35 mm SS ferrule with a thermocouple (K-type, NTT Heating, Sdn Bhd, Selangor, Malaysia) connected to a computer via pico data logger. Before the set-up, 30 g of crude pyrolytic oil was mixed with a certain amount of catalyst in a closed container and charged into the reactor after the bottom the reactor was sealed off. The system was purged with nitrogen (99.9% purity, Linde Gases Sdn. Bhd) for about two minutes and the fittings were assembled. The reactor was heated electrically at 50 °C/min. After the temperature attained the set-value and the required reaction time is reached, the power was switched off and the system was allowed to cool to room temperature. Subsequently, the valve was opened for gas collection and the reactor with remaining content was weighed. The reactor content was carefully collected in a container. Phase separation was carried out using centrifuge (Eppendorf™ 5430, Fisher Scientific Sdn. Bhd. Selangor, Malaysia) at 6500 rpm for 12 min. Aqueous phase and organic liquid product were separated and weighed. Samples were withdrawn for further analysis. The reactor was thoroughly washed with excess acetone and all its contents were recovered and mixed with remaining content (solid and tar) in the centrifuge tube. Solids in the mixture were separated using vacuum filtration with the aid of sartolon polyamide filter paper (0.45 μm pore size) and washed with acetone and oven dried at 60 °C overnight. The total liquid, organic, aqueous, solid and gas yield were computed using equations below. The experiment was carried out in triplicates and standard deviations were computed.

$$W_{TLP} = (W_{R2} - W_{R1}) + W_{ACQ} - W_{TSLD} \quad (1)$$

$$Yield (\%)_{TLP} = \left[\frac{W_{TLP}}{W_{RBO}} \right] \times 100 \quad (2)$$

$$Yield (\%)_{ACQ} = \left[\frac{W_{ACQ}}{W_{RBO}} \right] \times 100 \quad (3)$$

$$Yield (\%)_{OLP} = Yield (\%)_{TLP} - Yield (\%)_{ACQ} \quad (4)$$

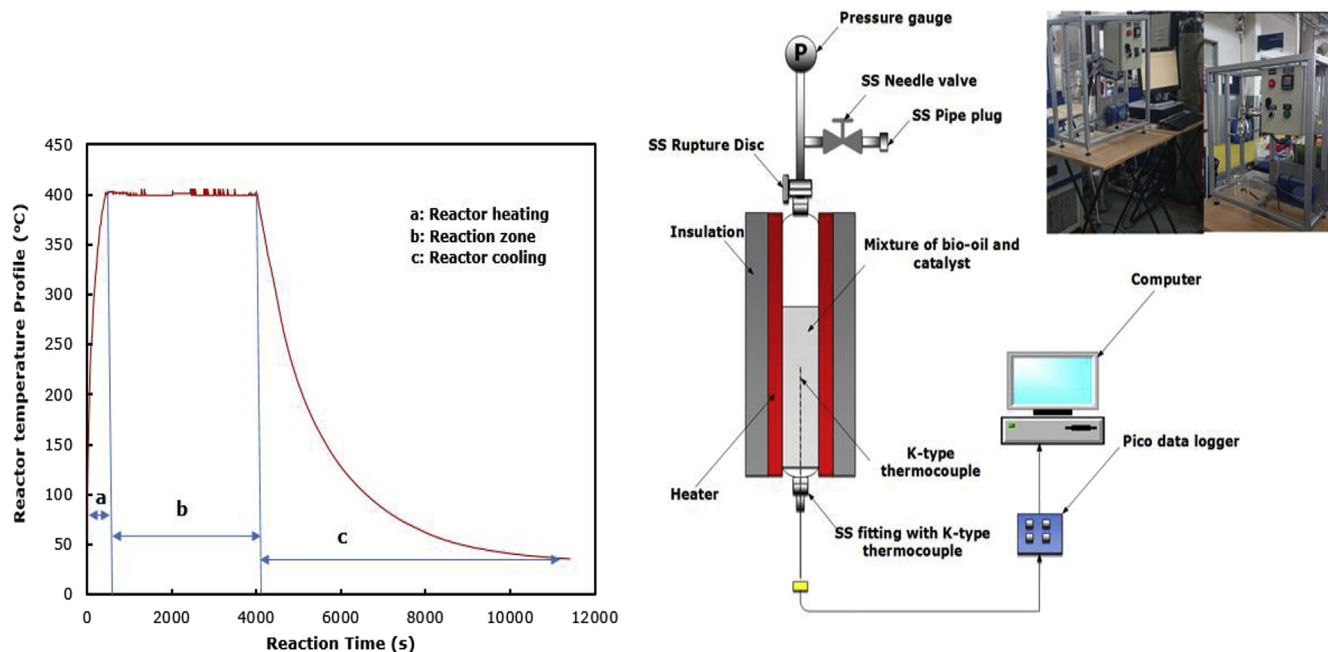


Fig. 1. Schematic diagram of experimental set-up of pyrolytic oil deoxygenation.

$$\text{Yield } (\%)_{SLD} = \left[\frac{W_{TSLD} - W_{IC}}{W_{RBO}} \right] \times 100 \quad (5)$$

$$\text{Yield } (\%)_{GP} = 100 - \{ \text{Yield } (\%)_{TLP} + \text{Yield } (\%)_{SLD} \} \quad (6)$$

where W is weight in gram and the subscript TLP, R₂, R₁, RBO, ACQ, OLP, TSLD, SLD, IC and GP represent total liquid product, reactor and its content, empty reactor, raw pyrolytic oil, aqueous phase, organic liquid product, total solid product, solid yield, initial catalyst and gas product respectively.

2.3. Product characterization

Characterization of the liquid product was carried out. Higher heating value was determined using an oxygen bomb calorimeter (Parr 6100, Parr Instruments, Molin, USA). Elemental compositions were determined using a CHNS/O analyzer (2400 Series II CHNS/O analyzer, Perkin Elmer Sdn Bhd, Selangor, Malaysia). Fractionation of the organic phase pyrolytic oil was simulated using TGA in nitrogen atmosphere at 20 mL/min, 10 °C/min from ambient to 500 °C to examine the volatile fractions and the result was compared with the simulated distillation of fossil-gasoline, kerosene and diesel. Chemical composition of the pyrolytic oil was determined using a gas chromatograph-mass spectrometer (GC-MS) system (PerkinElmer Clarus® SQ 8, Akron, USA) with a quadruple detector and PerkinElmer-Elite™-5ms column (30 m × 0.25 mm × 0.25 μm) (PerkinElmer, Akron, USA). The oven was programmed at an initial temperature of 40 °C, ramp at 5 °C/min to 280 °C and held there for 20 min. The injection temperature, volume, and split ratio were 250 °C, 1 μL, and 50:1 respectively. Helium was used as carrier gas at 1.0 mL/min. MS ion source at 250 °C with 70 eV ionization energy was used. Peaks of the chromatogram were identified by comparing with standard spectra of compounds in the National Institute of Standards and Technology (NIST, Gaithersburg, MD, USA) library. The gas products collected in a gas sample bag (Tedlar, SKC Inc., USA) was analyzed using a gas chromatography (PerkinElmer Clarus 500, Akron, USA) equipped with a stainless steel column

(Poropak R 80/100) and thermal conductivity detector (TCD). Helium was used as a carrier gas and the GC was programmed at 60 °C, 80 °C and 200 °C for oven, injector and TCD temperature, respectively.

3. Results and discussion

3.1. Characteristics of the catalysts

The diffractogram of the catalysts is shown in Fig. 2a. Both the parent ZSM-5 and the alkaline treated samples exhibited main peaks at around 2θ between 20° and 25°, which are typical characteristic peaks for ZSM-5. Although the intensity of the modified zeolite (0.2HZSM-5 and 0.3HZSM-5) decreased with increased NaOH concentration. This observation shows a loss of crystallinity due to desilication which could also be linked to the formation of mesoporous structures in the material (Alaba et al., 2016b). Physisorption analysis (Fig. 2b) of ZSM-5 displayed a type I isotherm according to the IUPAC classification. The isotherm showed a very strong adsorption in the initial region and a plateau at high relative pressure (>0.9). This pattern indicates that ZSM-5 is a microporous material (Ibáñez et al., 2014). Both 0.2HZSM-5 and 0.3HZSM-5 displayed a combination of type I and IV isotherms with a low slope region at the middle that shows the presence of few multilayers and a hysteresis loop at relative pressures above 0.4, which could be linked to capillary condensation in a mesoporous material (Li et al., 2014a). With increasing NaOH concentration, the hysteresis loop became more pronounced and could also be related to the level of mesoporous structure formed in the sample after the desilication. Other characteristics of catalysts from the physisorption analysis are summarized in Table 1. Comparing ZSM-5 and modified ZSM-5, as expected, the Si/Al ratio decreased between 34 and 40% after desilication. Similarly, reduction in Brunauer Emmet Teller (BET) specific surface area (S_{BET}), S_{micro} and V_{micro} were also observed in the modified ZSM-5. This observation shows that some of the micropores in the parent ZSM-5 have been converted to mesoporous structures after the desilication, which have contributed to the resulting mesoporosity in the modified ZSM-5 (Na et al., 2013). Pore

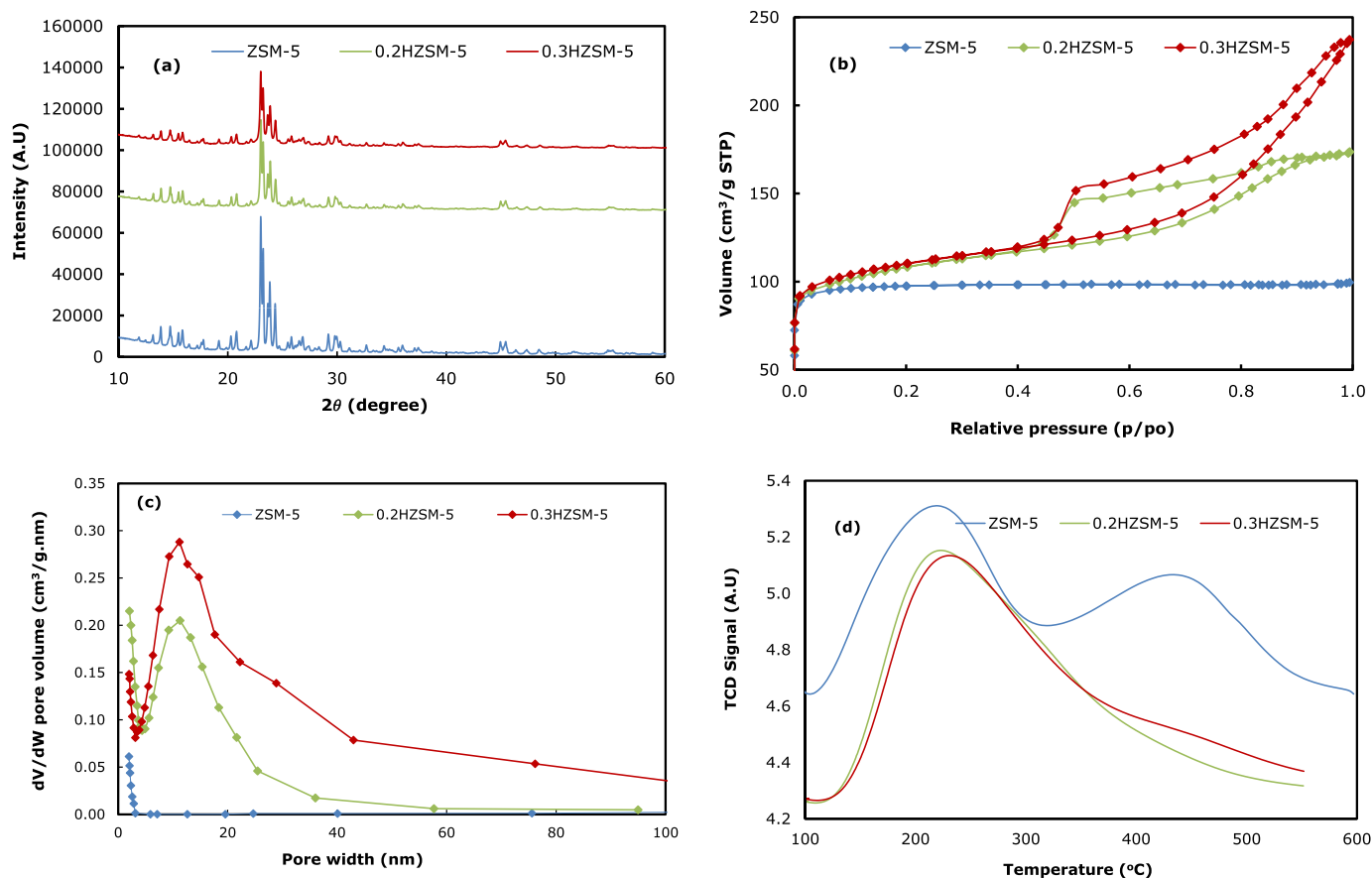


Fig. 2. Characteristics of ZSM-5 and Modified ZSM-5. (a) XRD diffractogram, (b) Isotherms of N₂ adsorption/desorption, (c) BJH Pore size distribution (d) NH₃-TPD temperature-programmed desorption curves analysis.

size distribution from Barrett, Joyner and Halenda (BJH) desorption plot (Fig. 2c) shows that bulk ZSM-5 has pore size of 2–3 nm while the modified 0.2HZSM-5 and 0.3HZSM-5 had pore size of 3–43 nm. Generally, microporous solids have pore size below 2 nm while pore size of 2–50 nm are characteristics of mesoporous solids (Storck et al., 1998). Consequently, the pore size exhibited by the bulk zeolite could be ascribed to the presence of larger micropores while that observed in the modified zeolites is an evidence of presence of mesoporous structures formed as a result of desilication. NH₃-TPD analysis (Fig. 2d) displayed two peaks in the parent ZSM-5 at temperatures around 219 and 435 °C while single peaks around 206 and 258 °C were observed 0.2HZSM-5 and 0.3HZSM-5 respectively. The high temperature peak represents the desorption of NH₃ from strong acid sites while those observed at temperatures between 206 and 258 °C are ascribed to the desorption of NH₃ from

weak acid sites (Saad et al., 2015). Disappearance of the strong acid sites in the modified ZSM-5 is attributed to decreased silica content in the respective samples (Na et al., 2013). Total surface acidity obtained from the area under each peak was found to be 3.8085, 3.0036 and 2.9635 mmol/g for ZSM-5, 0.2HZSM-5 and 0.3HZSM-5. The SEM-EDX (Fig. 3) revealed that ZSM-5 is highly crystalline, with hexagonal prismatic morphology and different particle size of less than 500 nm. Both 0.2HZSM-5 and 0.3HZSM-5 had morphological characteristic similar to the parent ZSM-5 indicating that the morphological integrity of the catalyst was not affected by desilication.

3.2. Products distribution and characterization

Fig. 4 presents catalytic performance of ZSM-5 and modified

Table 1

Treatment condition and characteristics of zeolite.

Catalyst	C _{NaOH} (mol/L)	(Si/Al) ^a (mol/mol)	(S _{BET}) ^b surface area (m ² /g)	(S _{micro}) ^c	(S _{meso}) ^d	(V _{micro}) ^c volume (cm ³ /g)	(V _{meso}) ^d	total acidity (mmol/g)
ZSM-5	0.00	20.76	385.20	356.54	11.67	0.14	0.01	3.81
0.2HZSM-5	0.20	13.79	369.43	274.66	115.55	0.10	0.17	3.00
0.3HZSM-5	0.30	12.51	374.88	240.23	175.09	0.11	0.28	2.96

^a Determined by X-ray fluorescence.

^b Brunauer–Emmett–Teller (BET) method.

^c t-plot method.

^d Barrett, Joyner and Halenda (BJH) method.

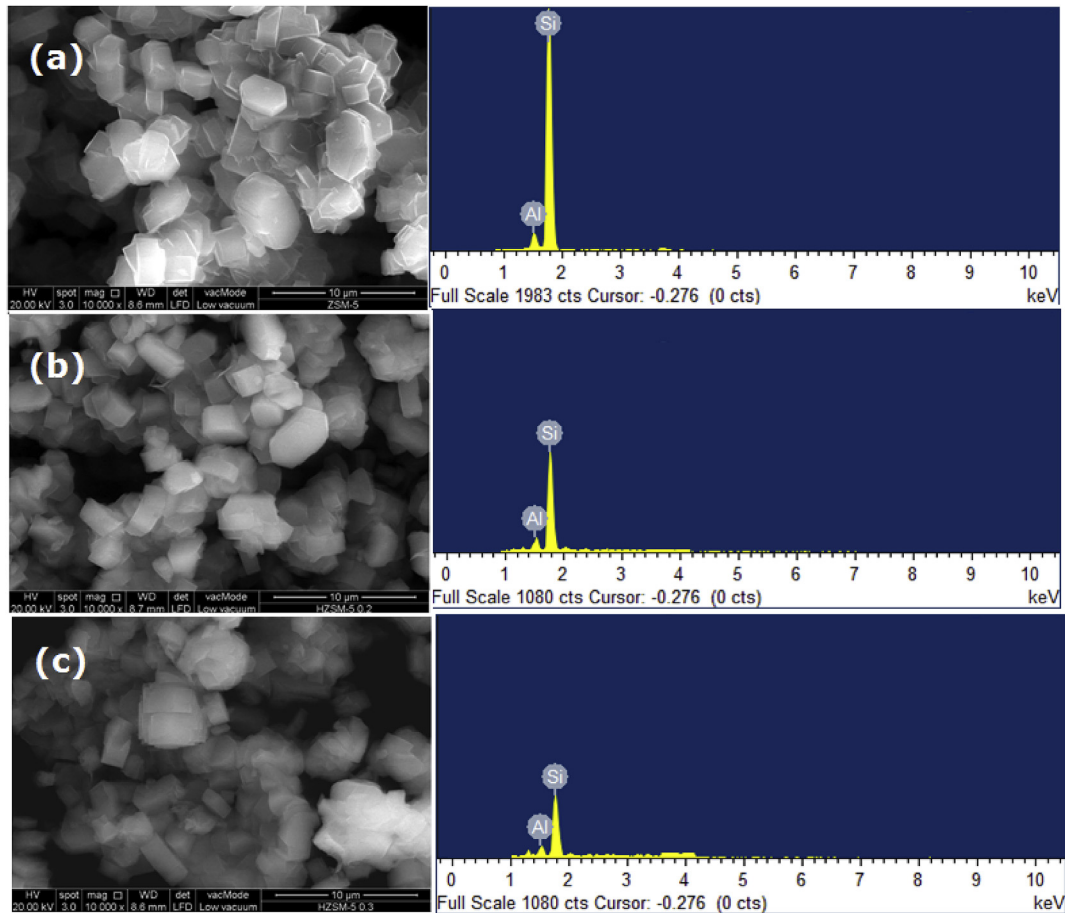


Fig. 3. SEM-EDX images of (a) ZSM-5, (b) 0.2HZSM-5 and (c) 0.3HZSM-5.

ZSM-5 in the upgrading of pyrolytic oil under 60 min reaction time at 400 °C and catalyst loading of 2.0 wt%. Thermal condition (0.0 wt % catalyst loading) was used as control. Under this condition, total liquid, non-condensable gas and solid product collected was 76.6, 22.5 and 0.9 wt%. The total liquid yield decreased to 51.10, 50.30 and 47.40 wt% while the non-condensable gas increased to 32.90, 37.10 and 43.30 wt% when ZSM-5, 0.2HZSM-5 and 0.3HZSM-5 was applied respectively. The lower liquid yield and increased gas

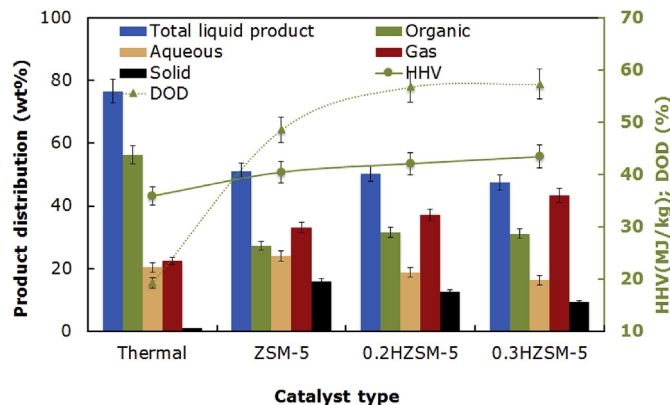


Fig. 4. Effect of catalyst on deoxygenation of bio-oil at 400 °C. Feed: 30 g pyrolytic oil, catalyst loading: 2.0 wt%. Solid: char and tar. Values are the means (n = 3).

production with the catalysts is attributed to several catalytic reactions such as decarbonylation and decarboxylation (Mohammed et al., 2016). Increase in solid product was recorded with the catalysts relative to the control. Comparing between the catalysts, ZSM-5 produced highest solid product (16.0 wt%) while 0.3ZSM-5 had lowest solid yield (9.30 wt%). Vitolo et al. (2001) reported total solid content of about 11.0 wt% during upgrading of pyrolysis oil over ZSM-5. Similarly, in a separate study by Saad et al. (2015), a total solid content of 29.2 wt% was recorded. The high yield of solid with ZSM-5 is attributed diffusion resistance of large oxygenated compounds or coke precursors in the raw pyrolytic oil, which undergo polymerization and polycondensation reactions and finally deposited on the catalyst surface. Consequently, the lower solid yield recorded with modified ZSM-5 can be linked to the improved pore structures in the modified ZSM-5. This observation is contrary to the report of Puértolas et al. (2015). The authors observed increase in solid yield and reduction in total liquid product over the hierarchical zeolites. However, this dissimilarity could be attributed to difference in pore and acidity of the hierarchical zeolites. Mesoporous ZSM-5 produced 15–16% higher organic phase and 21–32% lower aqueous phase compared to the bulk ZSM-5. This observation indicates that bulk ZSM-5 favored dehydration reaction while the modified ZSM-5 promoted more decarbonylation and decarboxylation, which substantiated the higher gas yield recorded with the modified catalyst. Higher heating value (HHV) of the organic phase (Fig. 4) increased from 29.18 MJ/kg (raw pyrolytic oil dry basis) to 35.90 MJ/kg after the thermal treatment, which accounted for about 23% increase. Increase in the HHV was also

recorded after catalytic treatment. Upgrading over ZSM-5, 0.2HZSM-5 and 0.3HZSM-5 produced organic phase with HHV of 40.46, 42.08 and 43.43 MJ/kg respectively. These values accounted 39–49% increase in the HHV relative to the raw pyrolytic oil. Degree of deoxygenation (DOD) (Fig. 4) calculated using Equation (7) was 19.24% after thermal treatment, which increased significantly to 48.58% with ZSM-5. The modified ZSM-5 produced more deoxygenated organic phase with DOD of about 57%. The high DOD recorded with the catalysts is therefore responsible for the improved HHV.

$$\text{DOD (\%)} = \left[\frac{O_j - O_i}{O_i} \right] \times 100 \quad (7)$$

where O_j and O_i represent oxygen content of upgraded pyrolytic oil and raw pyrolytic oil on dry basis respectively.

Puértolas et al. (2015) reported 34% DOD of pyrolytic oil over bulk ZSM-5 while higher DOD recorded with hierarchical mesoporous ZSM-5 was 42%. Maximum HHV of 35.3 MJ/kg was recorded, which was attributed the higher DOD achieved with the mesoporous ZSM-5. Similar improvement in DOD and HHV of upgraded pyrolytic oil over mesoporous ZSM-5 has been reported by Veses et al. (2016). The authors recorded 7.1% DOD with thermal upgrading while 39% DOD was recorded with mesoporous ZSM-5. The corresponding HHV was 27.3 and 32.5 MJ/kg. Other physicochemical properties of pyrolytic oil are summarized in Table 2. There was no clear trend in pH value of the upgraded pyrolytic oil. Although, slight decrease in acidity of the upgraded pyrolytic oil was observed (3.88–3.92) relative to the raw pyrolytic oil (3.71) except for the thermally upgraded pyrolytic oil, which had pH value of 3.6. The decrease in the acidity of the oil produced over the catalyst is an indication of reduction of organic acids and phenolic compound through carboxylation and decarbonylation reactions (Mohammed et al., 2016).

Thermogravimetric analysis of pyrolytic oil provides data on weight loss by evaporation as sample is heated over a certain temperature range. The resulting information similar to the distillation data, which can be used to estimate amount of pyrolytic oil that will distil into specific fuel products. In this study, TGA analysis of commercial fossil premium motor spirit (PMS), kerosene and diesel was performed as standard. Organic raw pyrolytic oil feedstock and upgraded samples were subjected to the same thermal treatment. From Fig. 5a, final evaporation temperature of PMS, kerosene and diesel was found to be 126, 185 and 291 °C respectively. Using the final evaporation temperature, by extrapolation, the raw organic pyrolytic oil constitutes (Fig. 5b) nearly 70 wt% volatile fraction. The weight loss above 300 °C can be attributed to thermal decomposition of residue. About 68 wt% of the oil had boiling range similar to that of diesel. Similarly, approximately 48 wt% of the pyrolytic oil is made up of kerosene boiling fraction while 35 wt% had boiling characteristic comparable to that of PMS.

Evaporation profile of thermally upgraded pyrolytic oil revealed increase in diesel and kerosene boiling fractions to 75 and 50 wt% while volatile fraction with PMS boiling characteristics decreased to 31 wt% relative to the raw pyrolytic oil. Upgraded pyrolytic oil over bulk ZSM-5 had about 77, 53 and 34 wt% diesel, kerosene and PMS boiling fraction respectively. Reduction in PMS boiling fraction recorded with thermal and ZSM-5 compared to the raw pyrolytic oil could be attributed to thermal and catalytic cracking of light fractions originally present in the pyrolytic oil feedstock. Pyrolytic oil upgrading over modified ZSM-5 produced about 78–84 wt%, 57–67 wt% and 43–50 wt% volatile organic fraction with boiling point comparable to that of diesel, kerosene and PMS respectively. The increased volatile fraction recorded with modified ZSM-5 could be ascribed to cracking of heavy molecular fractions and subsequent transformation.

3.3. GC-MS analysis of organic phase

Compounds identified in the raw and upgraded pyrolytic oil are grouped into hydrocarbons (HC), aromatic hydrocarbons (ARHC), methoxy aromatics (MARHC), phenol (PHOL), methoxy phenol (MPHOL), acids, aldehydes and ketones (AAK), methylester (MEST) and other value added chemicals (OVAC). The amounts of each component is expressed in percentage (%) based on the relative area from GC-MS analysis as summarized in Table 3. Noticeable changes were observed in the composition of the upgraded pyrolytic oil. Increase in PHOL content was recorded in thermally upgraded pyrolytic oil relative to the raw pyrolytic oil. This is ascribed to thermal decomposition of MPHOL which decreased considerably. The process involves formation of methyl radical resulting in hydroxyphenoxy radical, which subsequently decarboxylates to cyclopentadienyl radical. Radical-radical reaction between methyl and cyclopentadienyl lead to the formation of phenols (Scheer et al., 2011). High formation of phenol has also been reported by Veses et al. (2016). The authors recorded about 21.32% phenol content in the blank test relative to 14.66–18.41% obtained with catalyst. Thermal cracking of MPHOL to MARHC may have occurred, which is responsible to the increased composition of MARHC in the thermally upgraded pyrolytic oil relative to the feedstock and other upgraded oil. Significant reduction in AAK was also recorded with thermal cracking. Similarly, the percentage of hydrocarbon (1,3-dimethyl-1-cyclohexene) in the feedstock increased from 4.67 to 5.2% but a new hydrocarbon structure, 1,3,5-cycloheptatriene was observed after the upgrading. Benzene originally present in the feedstock was not detected in the product after thermal treatment. Therefore, cycloheptatriene may have originated from transformation of benzene and the cyclohexene and subsequent rearrangement and ring expansion. Pyrolytic oil upgraded over bulk ZSM-5 and modified ZSM-5 produced oil with less PHOL, AAK and complete elimination of MPHOL through series of reactions such as dehydration, decarbonylation and

Table 2
Physicochemical properties of raw and upgraded pyrolytic oil.

Property	Raw	Thermal	ZSM-5	0.2HZSM-5	0.3HZSM-5
Density (g/cm ³)	0.98 ± 0.0	0.95 ± 0.0	0.91 ± 0.0	0.9 ± 0.0	0.9 ± 0.0
pH	3.71 ± 0.01	3.6 ± 0.01	3.92 ± 0.01	3.88 ± 0.01	3.92 ± 0.01
HHV (MJ/kg)	29.18 ± 0.10	35.90 ± 0.10	40.46 ± 0.10	42.08 ± 0.10	43.43 ± 0.10
C (wt %)	53.87 ± 1.71	60.93 ± 1.72	72.86 ± 1.70	74.82 ± 1.73	74.75 ± 1.72
H (wt %)	6.45 ± 0.07	7.50 ± 0.10	7.36 ± 0.09	8.62 ± 0.11	8.55 ± 0.10
N (wt %)	1.35 ± 0.01	1.10 ± 0.01	0.34 ± 0.01	0.39 ± 0.01	0.24 ± 0.01
S (wt %)	0.76 ± 0.01	0.13 ± 0.01	0.12 ± 0.01	0.14 ± 0.01	0.22 ± 0.01
O* (wt %)	37.57 ± 1.01	30.34 ± 1.01	19.32 ± 1.01	16.24 ± 1.01	16.03 ± 1.01

Value are the mean (n = 3) ± standard deviation.

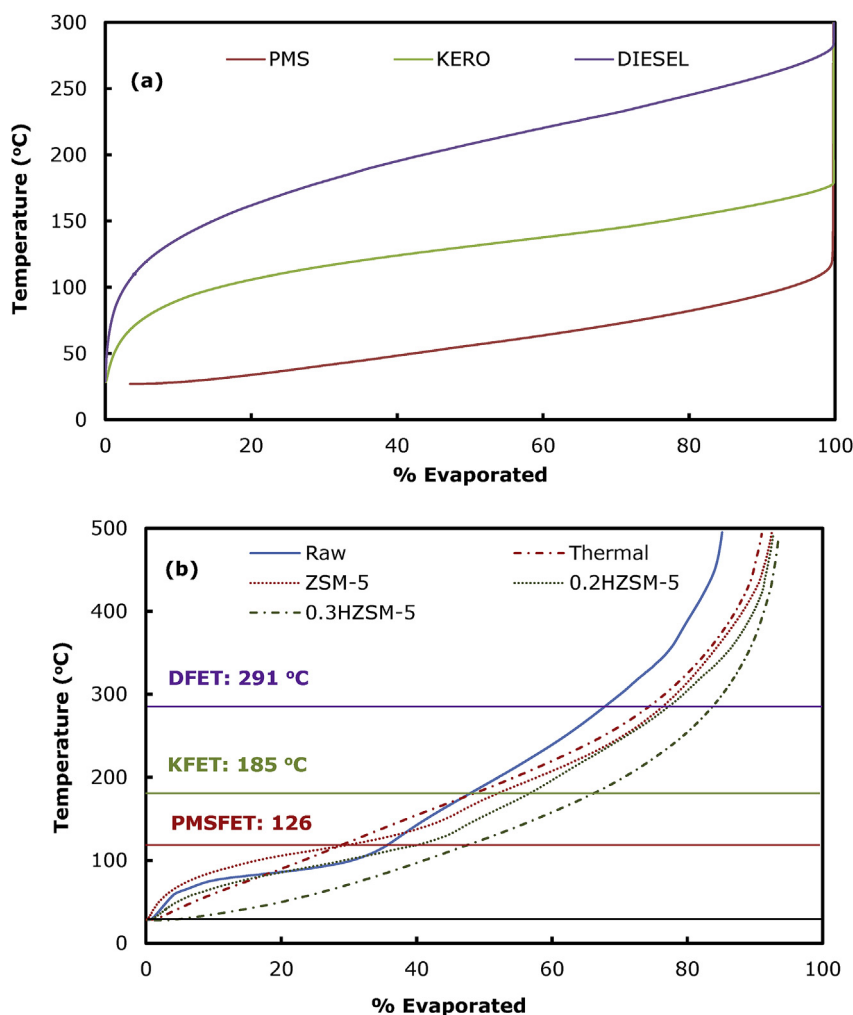


Fig. 5. Simulated distillation using TGA. (a) Premium motor sprit-PMS, kerosene and diesel (b) Raw and upgraded organic phase pyrolytic oil. DFET, KFET and PMSFET: diesel, kerosene and PMS final evaporation temperature.

decarboxylation. PHOL content in the upgraded oil over ZSM-5 increased by 47% and ARHC by a factor of five relative to the raw pyrolytic oil, which may be due to complete elimination MPHOL as rightly observed (Table 3). This suggests that conversion MPHOL proceeded via demethylation into phenol and subsequent dehydration into aromatics. Many studies have reported transformation MPHOL (guaiacol) into aromatics over ZSM-5. Studies by Cheah et al. (2016) on deoxygenation of hydroxyacetaldehyde and guaiacol catalyzed by HZSM-5 reported that conversion of guaiacol to

aromatic was through demethylation into phenol and subsequent dehydration into aromatics. Similar observations have been reported by Wei et al. (2016) and Zhang et al. (2016). The authors in their separate studies, stated that guaiacol and furan compounds were transformed into aromatics over ZSM-5. However, from the composition of MARHC in the upgraded pyrolytic oil over ZSM-5 (Table 3), which increased by about 63% relative to the MARHC content in the raw pyrolytic oil. It can be seen that conversion of MPHOL is not a simple reaction due to complex nature of the raw pyrolytic oil. Consequently, based on the result obtained in this study, it can be stated that MPHOL is converted into aromatics via multi-reaction pathways. Modified ZSM-5 produced high amount of aromatics relative to parent ZSM-5, suggesting high degree of conversion of MARHC while formation of other HC compounds declined with hierarchical mesoporous ZSM-5. It is interesting to note that most of the HCs produced with parent ZSM-5 are cyclic olefins, which decreased with modified ZSM-5. Selectivity of olefins and aromatics by the catalysts is shown Fig. 6. It can be seen that the parent ZSM-5 produced more olefins and polyaromatic hydrocarbon (PAH) while the opposite trend was recorded with the modified ZSM-5. It can therefore be inferred that the high amount of solid earlier recorded with the parent ZSM-5 was due to evolution of PAH at acid sites, which serves as coke precursors and eventually result in the solid yield. Furthermore, the nature of

Table 3
Group of organic compound in the deoxygenated pyrolytic oil identified by GC-MS.

Composition (%)	Raw	Thermal	ZSM-5	0.2HZSM-5	0.3HZSM-5
HC	4.67	5.20	20.67	13.56	3.94
ARHC	2.53	0.00	13.33	20.40	26.87
MARHC	2.18	10.34	3.56	0.00	0.00
PHOL	28.15	65.91	41.25	43.12	47.70
MPHOL	37.87	5.03	0.00	0.00	0.00
AAK	16.88	4.35	12.69	3.71	2.01
MEST	4.68	9.18	8.50	11.75	11.00
OVAC	3.05	0.00	0.00	7.46	8.48

(HC) hydrocarbons, (ARHC) aromatic hydrocarbons, (MARHC) methoxy aromatic hydrocarbons, (PHOL) phenol, (MPHOL) methoxy phenol, (AAK) acids, aldehydes and ketones, (MEST) methylester and (OVAC) other value added chemical.

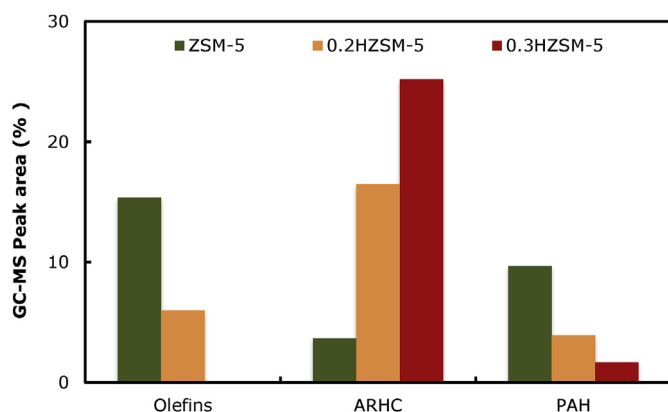


Fig. 6. Selectivity of olefins and aromatic hydrocarbons.

aromatics recorded with modified ZSM-5 were mainly alkyl benzenes, which suggests that hierarchical mesoporous ZSM-5 favored ring alkylation reaction. This trend seems to have correlation with Si/Al ratio. With decreasing Si/Al ratio, more alkyl benzenes were produced. Similar observation has been reported by Foster et al. (2012). The authors observed that decrease in Si/Al ratio promote production of aromatics. They also reported that mesoporous ZSM-5 favored the production of alkylated monoaromatic hydrocarbons. It worthy to note that the content of esters (MEST) in the raw pyrolytic oil increased significantly in all the upgraded pyrolytic oil. MEST in the upgraded oil over bulk ZSM-5 is similar to the MEST content of the thermally upgraded oil. It is possible that some small organic molecules generated during the catalytic cracking of pyrolytic oil with ZSM-5 which would otherwise transesterify during quenching of reaction system may have polymerised, resulting in solid formation as rightly observed in the product distribution above. Similar observation has been reported by Cheng et al. (2014) during catalytic cracking of crude pyrolytic oil in a high-pressure reactor. The authors stated that formation of solid was promoted by ZSM-5 via polymerization of small compounds during the period of cooling down the reactor. On the other hand, the MEST in the upgraded oil over modified ZSM-5 was 20–28% higher relative to the MEST in the thermally upgraded oil. This suggests that some of the active chemical species during cracking were transesterified into methyl esters during quenching of the reactor. For example, decomposition of methanol-imidazole present in the raw pyrolytic oil to release methanol is expected, which could further react with organic acids to form esters. Methyl esters are biodiesel component, which is another valuable renewable product.

Most of the catalytic upgrading studies reported in the literature focused mainly on the upgraded organic phase product. Aqueous phase produced as a result of deoxygenation reactions is mostly regarded as a waste stream and its composition generally unknown. In this study, analysis of the aqueous phase from the catalytic upgrading of pyrolytic oil was carried out with GC-MS and the most abundant chemical species identified are summarized in Supplementary Table S1. Aqueous phase from ZSM-5 deoxygenation consist phenols, benzenediols, alcohols and small amount of acid, aldehyde and ketones while the aqueous phase resulting from mesoporous ZSM-5 were mostly ketones and aldehydes, phenols and traces of alcohols. These compounds are intermediate products of deoxygenation reactions and may be utilised as organic building blocks for synthesis of important fine chemicals. Conversion of water soluble renewable organic materials has been characterised with high conversion efficiency. Studies by Timko et al. (2006) on conversion and selectivity of a Diels-Alder cycloaddition by use of emulsions of carbon dioxide and water revealed that the reaction in

emulsions of water and carbon dioxide leads to the high selectivity and conversion that are characteristic of water. Consequently, aqueous phase from the catalytic upgrading of pyrolytic oil represent environmentally benign stream that can be used for production of valuable chemicals.

3.4. GC analysis of gas composition

Composition of gas as determined by the GC is summarized in Table 4. The component identified include hydrogen (H₂), carbon monoxide (CO), carbon dioxide (CO₂) and methane (CH₄). Thermal cracking produced gas with highest CH₄ content (33.42 vol%), suggesting production of small organic molecules. Similarly, significant amount of CO in the gas from thermal cracking is an evidence of some decarbonylation reaction, which confirmed the formation of cyclopentadienyl radical as previously stated in the mechanism of phenol formation from thermal decomposition of methoxyphenol. The principal composition of gas from the catalytic upgrading process were CO and CO₂, which are indications of decarboxylation and decarbonylation reactions. With modified ZSM-5, the CH₄ composition decreased relative to ZSM-5. This can be linked to the alkylation reaction observed with the hierarchical ZSM-5. It can therefore be stated that the alkyl group generated during upgrading reacted with the aromatic pool within the system and subsequently result in alkyl benzenes as observed in the previous section above. Furthermore, considerable increase in the amount of CO and CO₂ were recorded with the mesoporous ZSM-5 compared to bulk ZSM-5, indicating higher degree of decarboxylation and decarbonylation. This observation is in good agreement with the result of GC-MS analysis. Preferential decarbonylation and decarboxylation reactions with hierarchical mesoporous ZSM-5 has been reported in the literature (Veses et al., 2016). A summary of comprehensive material flow and possible reaction pathways during upgrading is shown in Figs. 7 and 8 respectively.

3.5. Reusability of modified ZSM-5

Stability of the hierarchical mesoporous ZSM-5 in the upgrading of pyrolytic oil was evaluated with 0.3HZSM-5, being the best performing catalyst observed in this study. Upgrading experiments were conducted in four consecutive cycles. After each experiment, the spent catalyst was regenerated in air at 550 °C for 6 h at 10 °C/min heating rate. A portion of the regenerated catalyst was subsequently characterised. Catalyst loading (wt%) and other reaction parameters were kept constant to ensure similar contact time. From Fig. 9, reusability of modified ZSM-5 showed no significant impact on the total liquid, gas and solid yields but rather have considerable impact on the production of organic and aqueous phases. First cycle produced 29.5 wt% organic phase, which decreased to 25 wt% in the second cycle. The corresponding aqueous phase recorded was 10.6 wt% and 16.9 wt%. There was no significant difference between organic yield in the second and third cycles but thereafter decreased to 21.2 wt% in the fourth cycle. Increase in the aqueous phase was recorded after each cycle. This observation suggests that regenerated catalyst promoted dehydration reaction. From the physicochemical analysis, a continuous

Table 4
Gas composition from GC-TCD analysis.

Composition (vol %)	Thermal	ZSM-5	0.2HZSM-5	0.3HZSM-5
H ₂	1.35	1.61	1.51	1.42
CH ₄	33.42	24.66	17.14	12.18
CO	25.34	27.72	32.92	36.88
CO ₂	9.03	28.01	30.43	32.35

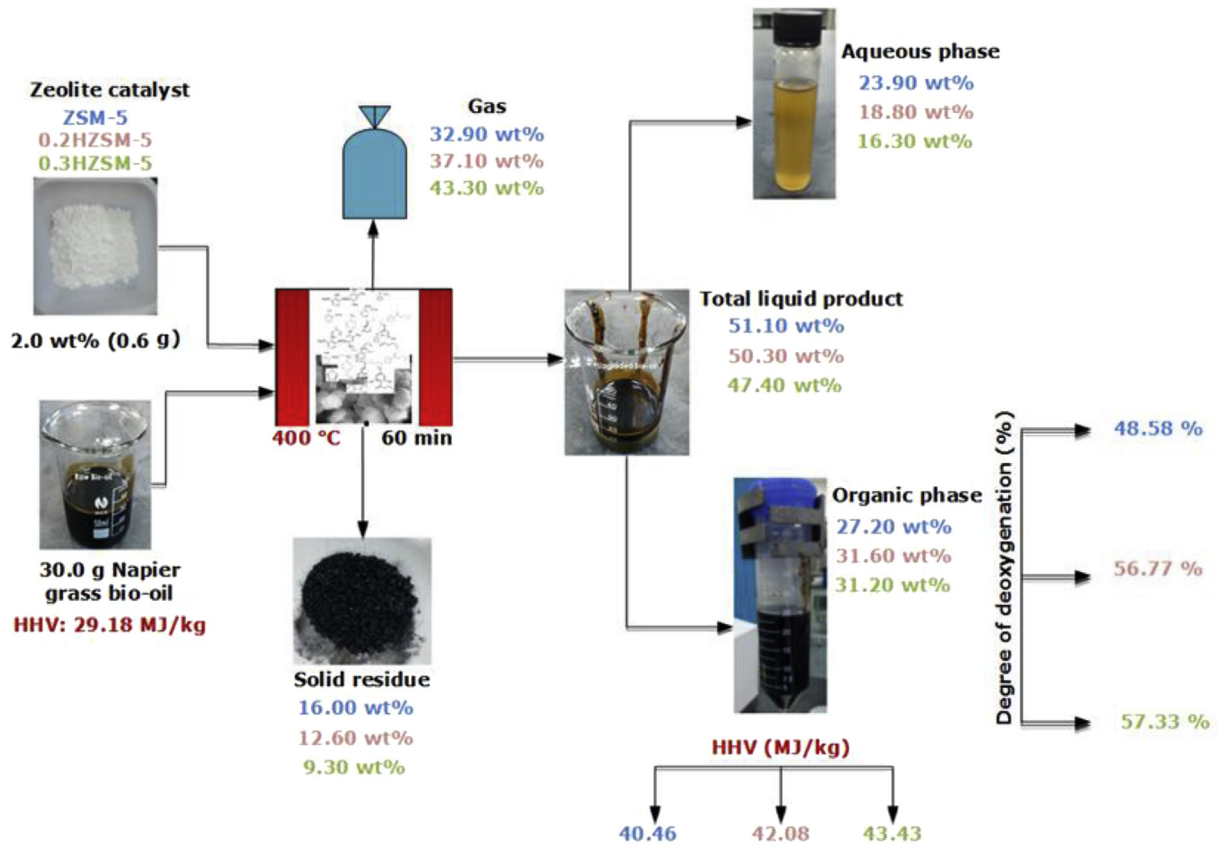


Fig. 7. Summary of material, heating value and degree of deoxygenation.

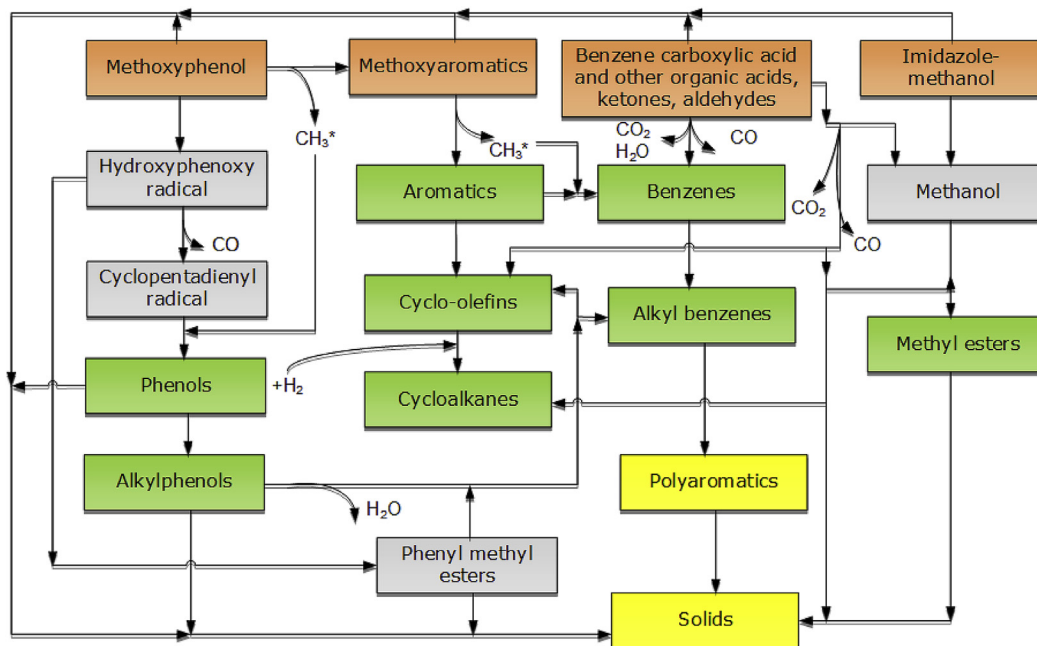


Fig. 8. Possible reaction pathways of thermal and catalytic ex-situ upgrading of pyrolytic oil. ■ Component in the raw pyrolytic oil, ■ intermediate products, ■ desired products, ■ undesired products.

decline in HHV and DOD were observed with catalyst in the consecutive cycles (Fig. 9), which are indications of loss of catalytic activity probably due to chemisorption of poisons such as nitrogen

or sulfur containing compounds on the active sites (Argyle and Bartholomew, 2015). Puértolas et al. (2015) reported that the ratio of organic to aqueous phase in the upgraded pyrolytic oil over

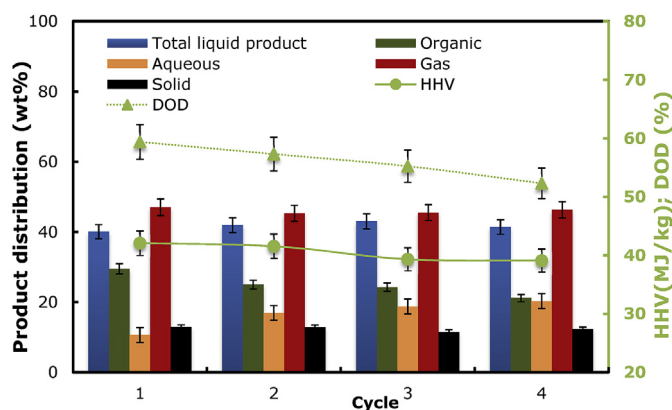


Fig. 9. Reusability of 0.3HZSM-5 on deoxygenation of pyrolytic oil at 400 °C. Catalyst loading (catalyst/pyrolytic oil): 4.0 wt%.

regenerated mesoporous ZSM-5 decreased and was attributed to decrease in the acid sites. Chemical composition of upgraded pyrolytic oil and gas collected over regenerated catalyst are summarized in Table 5 and Table 6 respectively. In consistent with the physicochemical properties, significant decrease in ARMHCs was observed in the pyrolytic oil after each cycle with corresponding increase in PHOL content. AAK and MARHC compounds were detected in the upgraded oil after the first cycle. From the gas analysis result (Table 6), a decline trend in the CO contents was observed after each cycle, which is an evidence of decreased decarbonylation reaction. Characteristics (BET XRD and SEM-EDX) of fresh and regenerated catalyst are shown in Table 7 and Fig. 10. From the physisorption analysis result (Table 7), all the properties of the regenerated catalyst decreased after four consecutive cycles except for the mesopore surface area which increased by 12%. BET surface area decreased by 44% while micro surface area and pore volumes decreased approximately three-folds lower relative to the original value. SEM-EDX images (Fig. 10b) displayed new peak for carbon and sulfur, suggesting thermal and chemical deactivation. As earlier stated, sulfur containing compounds are among the chemical species that result in catalyst poisoning. After regeneration, the catalyst composition was similar to that of fresh catalyst (Fig. 10c). Although the SEM image showed some disruption of original hexagonal prismatic structure in the regenerated catalyst, which is an indication of partial collapse in the catalyst morphology. This observation could be responsible for the reduction in surface and pore characteristics recorded. Similarly, the diffractogram (Fig. 10d) of the regenerated catalyst after four consecutive cycles displayed characteristic peaks similar to that of the fresh catalyst, indicating high stability. However, the peak

Table 5
Composition of upgraded pyrolytic oil (organic phase) over regenerated 0.3HZSM-5 catalyst.

Composition (%)	Cycle			
	1st	2nd	3rd	4th
HC	7.32	6.46	8.59	2.50
ARHC	40.94	25.40	12.58	10.42
MARHC	0.00	2.89	10.33	12.66
PHOL	44.70	50.12	62.28	63.32
MPHOL	0.00	0.00	0.00	2.46
AAK	0.00	3.38	2.81	5.03
MEST	7.04	11.75	3.41	3.61

(HC) hydrocarbons, (ARHC) aromatic hydrocarbons, (MARHC) methoxy aromatic hydrocarbons (PHOL) phenol, (MPHOL) methoxy phenol, (AAK) acids, aldehydes and ketones and (MEST) methyl ester.

Table 6
Gas composition from regenerated 0.3HZSM-5 catalyst.

Composition (vol %)	Cycle			
	1st	2nd	3rd	4th
H ₂	1.23	1.29	1.21	1.30
CH ₄	12.78	12.08	12.41	12.80
CO	35.22	33.78	30.44	29.53
CO ₂	31.87	30.01	30.82	28.77

Table 7
Characteristic of fresh and regenerated 0.3HZSM-5 after 4 cycle.

Catalyst	(S _{BET}) ^a	(S _{micro}) ^b	(S _{meso}) ^c	(V _{micro}) ^b	(V _{meso}) ^c
	surface area (m ² /g)			volume (cm ³ /g)	
Fresh 0.3HZSM-5	374.88	240.23	175.09	0.11	0.28
Regenerated 0.3HZSM-5	208.95	88.47	192.55	0.05	0.09

^a Brunauer–Emmett–Teller (BET) method.

^b t-plot method.

^c Barrett, Joyner and Halenda (BJH) method.

intensities in the regenerated catalyst were considerably lower than that of the fresh catalyst. This mean that crystallinity of 0.3HZSM-5 decreased with reusability. Therefore, the decline in the catalyst performance recorded after each cycle can be attributed to the changes in its properties, particularly the surface area, which is directly proportional to the number of active sites. Similar observations have been reported in literature (Vitolu et al., 2001; Puértolas et al., 2015).

4. Conclusion

Ex-situ upgrading of pyrolytic oil derived from Napier grass over micro and hierarchical mesoporous ZSM-5 was carried out in a high-pressure reactor. Hierarchical mesoporous ZSM-5 (0.2HZSM-5 and 0.3HZSM-5) used in this study was produced through desilication of bulk ZSM-5 with aqueous sodium hydroxide solution. To understand the effect of catalyst in the upgrading process, thermal cracking was performed. Upgrading over microporous ZSM-5 produced 16.0 wt% solid, 27.2 wt% organic phase and 23.9 wt% aqueous phase liquid while modified zeolites produced 21–42% less solid and 15–16% higher organic phase liquid. Higher degree of deoxygenation of pyrolytic oil (57%) was achieved with the modified ZSM-5 relative to 48.58% recorded with bulk ZSM-5. GC-MS analysis of organic phase collected after catalytic upgrading revealed high transformation of methoxyphenol and methoxyaromatics. Bulk ZSM-5 produced cyclic olefins and polyaromatic hydrocarbons while modified ZSM-5 were selective toward cycloalkanes and alkylated monoaromatics, with significant reduction in polyaromatic production. Result of gas analysis showed that hierarchical mesoporous ZSM-5 favored decarboxylation and decarbonylation reactions compared to the bulk ZSM-5, which promoted dehydration reaction. 0.3HZSM-5 was found to be the best-performing catalyst and its reusability was tested over four consecutive cycles. Composition of aromatic hydrocarbon in the oil collected over regenerated catalyst decreased while increase in phenol content was recorded relative to the oil composition from the fresh catalyst. Furthermore, degree of deoxygenation and higher heating was found to decrease after each cycle, which was attributed to the loss catalyst active sites. This study demonstrated that pyrolytic oil derived from Napier grass could be transformed into that high-grade pyrolytic oil via catalytic upgrading over hierarchical mesoporous ZSM-5.

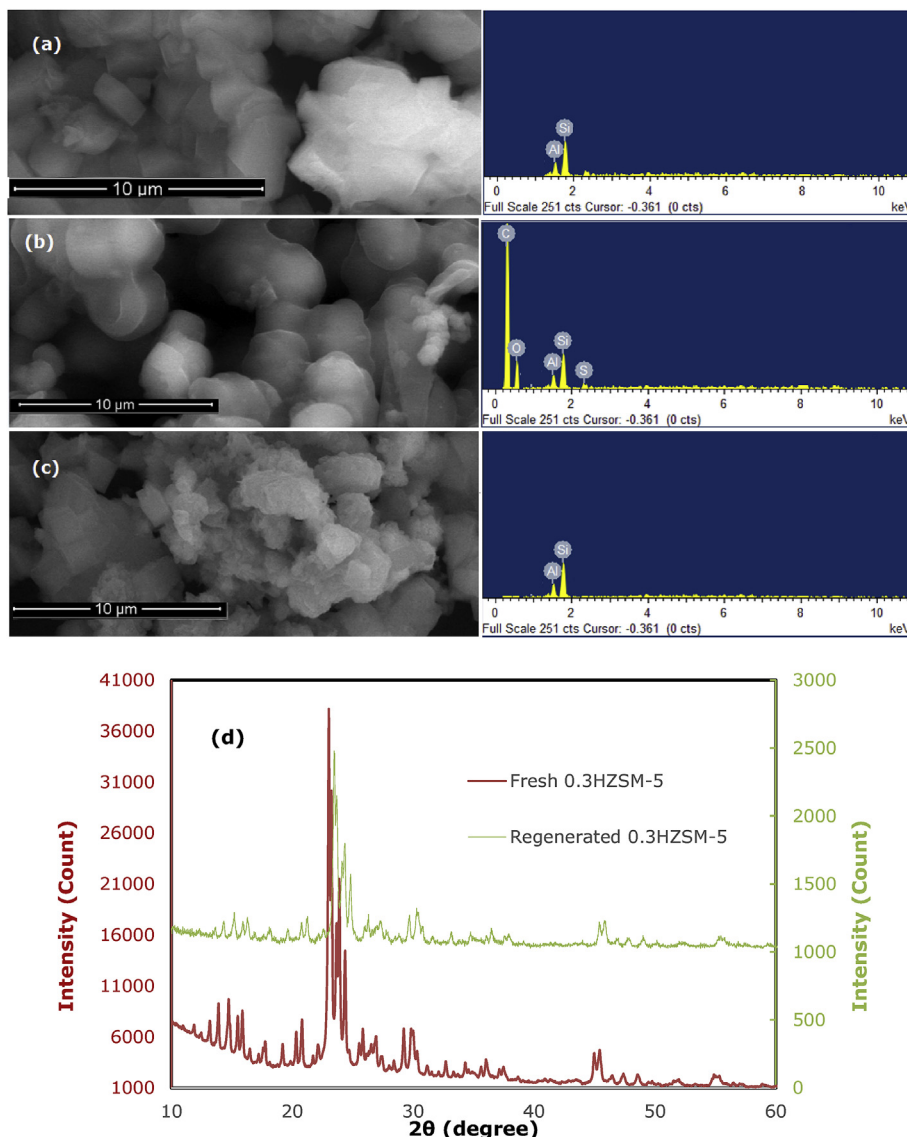


Fig. 10. Characteristics of 0.3HZSM-5 catalyst. SEM-EDX (a) fresh catalyst, (b) spent catalyst, (c) regenerated catalyst after 4 cycle, (d) diffractogram of fresh and regenerated sample.

Acknowledgment

The project was supported by the Crops for the Future (CFF) and University of Nottingham under the grant BioP1-005.

Appendix A. Supplementary data

Supplementary data related to this article can be found at <http://dx.doi.org/10.1016/j.jclepro.2017.06.105>.

References

- Alaba, P.A., Sani, Y.M., Mohammed, I.Y., Abakr, Y.A., Daud, W.M.A.W., 2016b. Synthesis and application of hierarchical mesoporous HZSM-5 for biodiesel production from shea butter. *J. Taiwan Inst. Chem. Eng.* 59, 405–412.
- Alaba, P.A., Sani, Y.M., Mohammed, I.Y., Daud, W., Ashri, W.M., 2016a. Insight into catalyst deactivation mechanism and suppression techniques in thermocatalytic deoxygenation of bio-oil over zeolites. *Rev. Chem. Eng.* 32 (1), 71–91.
- Argyle, M.D., Bartholomew, C.H., 2015. Heterogeneous catalyst deactivation and regeneration: a review. *Catalysts* 5, 145–269.
- Bischoff, H.W., Bold, H.C., 1963. *Phycological Studies. IV. Some Soil Algae from Enchanted Rock and Related Algal Species*. University of Texas Publications, pp. 1–95, 6318.
- Botas, J., Serrano, D.P., García, A., Ramos, R., 2014. Catalytic conversion of rapeseed oil for the production of raw chemicals, fuels and carbon nanotubes over Ni-modified nanocrystalline and hierarchical ZSM-5. *Appl. Catal. B* 145, 205–215.
- Cheah, S., Starace, A.K., Gjersing, E., Bernier, S., Deutch, S., 2016. Reactions of mixture of oxygenates found in pyrolysis vapors: deoxygenation of hydroxyacetaldehyde and guaiacol catalyzed by HZSM-5. *Top. Catal.* 59 (1), 109–123.
- Cheng, D., Wang, L.J., Shahbazi, A., Xiu, S., Zhang, B., 2014. Catalytic cracking of crude bio-oil from glycerol-assisted liquefaction of swine manure. *Energy Convers. Manag.* 87, 378–384.
- Foster, A.J., Jae, J., Cheng, Y.T., Huber, G.W., Lobo, R.F., 2012. Optimizing the aromatic yield and distribution from catalytic fast pyrolysis of biomass over ZSM-5. *Appl. Catal. A General* 423, 154–161.
- Gamliel, D.P., Cho, H.J., Fan, W., Valla, J.A., 2016. On the effectiveness of tailored mesoporous MFI zeolites for biomass catalytic fast pyrolysis. *Appl. Catal. A General* 522, 109–119.
- García, J.R., Bertero, M., Falco, M., Sedran, U., 2015. Catalytic cracking of bio-oils improved by the formation of mesopores by means of Y zeolite desilication. *Appl. Catal. A Gen.* 503, 1–8.
- Ibáñez, M., Artetxe, M., Lopez, G., Elordi, G., Bilbao, J., Olazar, M., Castaño, P., 2014. Identification of the coke deposited on an HZSM-5 zeolite catalyst during the sequenced pyrolysis-cracking of HDPE. *Appl. Catal. B* 148, 436–445.
- Lee, H.W., Park, S.H., Jeon, J.K., Ryoo, R., Kim, W., Suh, D.J., Park, Y.K., 2014. Upgrading of bio-oil derived from biomass constituents over hierarchical unilamellar mesoporous MFI nanosheets. *Catal. Today* 232, 119–126.
- Li, J., Li, X., Zhou, G., Wang, W., Wang, C., Komarneni, S., Wang, Y., 2014b. Catalytic fast pyrolysis of biomass with mesoporous ZSM-5 zeolites prepared by desilication with NaOH solutions. *Appl. Catal. A General* 470, 115–122.

- Li, T., Duan, A., Zhao, Z., Liu, B., Jiang, G., Liu, J., Wei, Y., Pan, H., 2014a. Synthesis of ordered hierarchically porous L-SBA-15 material and its hydro-upgrading performance for FCC gasoline. *Fuel* 117, 974–980.
- Mante, O.D., Agblevor, F., Oyama, S., McClung, R., 2014. Catalytic pyrolysis with ZSM-5 based additive as co-catalyst to Y-zeolite in two reactor configurations. *Fuel* 117, 649–659.
- Mohammed, I.Y., Abakr, Y.A., Kazi, F.K., 2017a. In-situ upgrading of Napier grass pyrolysis vapour over microporous and hierarchical mesoporous zeolites. *Waste Biomass Valorization* 1–14.
- Mohammed, I.Y., Abakr, Y.A., Yusup, S., Kazi, F.K., 2017b. Valorization of Napier grass via intermediate pyrolysis: optimization using response surface methodology and pyrolysis products characterization. *J. Clean. Prod.* 142, 1848–1866.
- Mohammed, I.Y., Abakr, Y.A., Kazi, F.K., Yusup, S., Alshareef, I., Chin, S.A., 2015. Comprehensive characterization of Napier grass as a feedstock for thermochemical conversion. *Energies* 8 (5), 3403–3417.
- Mohammed, I.Y., Kazi, F.K., Yusup, S., Alaba, P.A., Sani, Y.M., Abakr, Y.A., 2016. Catalytic intermediate pyrolysis of Napier grass in a fixed bed reactor with ZSM-5, HZSM-5 and Zinc-exchanged zeolite-a as the catalyst. *Energies* 9 (4), 246.
- Na, K., Choi, M., Ryoo, R., 2013. Recent advances in the synthesis of hierarchically nanoporous zeolites. *Microporous Mesoporous Mater.* 166, 3–19.
- Pérez-Ramírez, J., Mitchell, S., Verboekend, D., Milina, M., Michels, N.-L., Krumeich, F., Marti, N., Erdmann, M., 2011. Expanding the horizons of hierarchical zeolites: beyond laboratory curiosity towards industrial realization. *ChemCatChem* 3, 1731–1734.
- Puértolas, B., Veses, A., Callén, M.S., Mitchell, S., García, T., Pérez-Ramírez, J., 2015. Porosity–acidity interplay in hierarchical ZSM-5 zeolites for pyrolysis oil valorization to aromatics. *ChemSusChem* 8 (19), 3283–3293.
- Saad, A., Ratanawilai, S., Tongurai, C., 2015. Catalytic cracking of pyrolysis oil derived from rubberwood to produce green gasoline components. *BioResources* 10 (2), 3224–3241.
- Scheer, A.M., Mukarakate, C., Robichaud, D.J., Nimlos, M.R., Ellison, G.B., 2011. Thermal decomposition mechanisms of the methoxyphenols: formation of phenol, cyclopentadienone, vinylacetylene, and acetylene. *J. Phys. Chem. A* 115 (46), 13381–13389.
- Storck, S., Bretinger, H., Maier, W.F., 1998. Characterization of micro- and mesoporous solids by physisorption methods and pore-size analysis. *Appl. Catal. A General* 174 (1), 137–146.
- Tian, Q., Liu, Z., Zhu, Y., Dong, X., Saih, Y., Basset, J.M., Sun, M., Xu, W., Zhu, L., Zhang, D., Huang, J., 2016. Beyond creation of mesoporosity: the advantages of polymer-based dual-function templates for fabricating hierarchical zeolites. *Adv. Funct. Mater.* 26, 1881–1891.
- Timko, M.T., Allen, A.J., Danheiser, R.L., Steinfeld, J.I., Smith, K.A., Tester, J.W., 2006. Improved conversion and selectivity of a Diels–Alder cycloaddition by use of emulsions of carbon dioxide and water. *Ind. Eng. Chem. Res.* 45 (5), 1594–1603.
- Veses, A., Puértolas, B., López, J.M., Callén, M.S., Solsona, B., García, T., 2016. Promoting deoxygenation of bio-oil by metal-loaded hierarchical ZSM-5 zeolites. *ACS Sustain. Chem. Eng.* 4 (3), 1653–1660.
- Vitolo, S., Bresci, B., Seggiani, M., Gallo, M.G., 2001. Catalytic upgrading of pyrolytic oils over HZSM-5 zeolite: behaviour of the catalyst when used in repeated upgrading–regenerating cycles. *Fuel* 80 (1), 17–26.
- Wei, Y., Lei, H., Zhu, L., Zhang, X., Liu, Y., Yadavalli, G., Zhu, X., Qian, M., Yan, D., 2016. Hydrocarbon produced from upgrading rich phenolic compound bio-oil with low catalyst coking. *Fuel* 178, 77–84.
- Yakub, M.I., Abdalla, A.Y., Feroz, K.K., Suzana, Y., Ibraheem, A., Chin, S.A., 2015. Pyrolysis of oil palm residues in a fixed bed tubular reactor. *J. Power Energy Eng.* 3, 185–193.
- Zhang, B., Zhong, Z.P., Chen, P., Ruan, R., 2015. Microwave-assisted catalytic fast pyrolysis of biomass for bio-oil production using chemical vapor deposition modified HZSM-5 catalyst. *Bioresour. Technol.* 197, 79–84.
- Zhang, H., Luo, M., Xiao, R., Shao, S., Jin, B., Xiao, G., Zhao, M., Liang, J., 2014. Catalytic conversion of biomass pyrolysis-derived compounds with chemical liquid deposition (CLD) modified ZSM-5. *Bioresour. Technol.* 155, 57–62.
- Zhang, H., Wang, Y., Shao, S., Xiao, R., 2016. Catalytic conversion of lignin pyrolysis model compound-guaiacol and its kinetic model including coke formation. *Sci. Rep.* 6 <http://dx.doi.org/10.1038/srep37513>.